IEEE Access
Multidisciplinary ⋮ Rapid Review ⋮ Open Access Journal

Received 3 November 2025, accepted 17 December 2025, date of publication 19 December 2025,
date of current version 26 December 2025.

Digital Object Identifier 10.1109/ACCESS.2025.3646592

RESEARCH ARTICLE

An IEEE 2030.5-Based Legacy Protocol Converter for Interoperable DER Integration

CHANDRA SEKHAR CHARAN DANDE[1], DANIELE CARTA[2], (Member, IEEE), ERDEM GÜMRÜKCÜ[3], (Member, IEEE), ELYAS RAKHSHANI[4], (Senior Member, IEEE), ANDRES ACOSTA GIL[1], NITHIN MANUEL[1], ALEXANDRE LUCAS[5], ANDREA BENIGNI[2,6], (Senior Member, IEEE), AND ANTONELLO MONTI[1,7], (Senior Member, IEEE)

[1]Institute for Automation of Complex Power Systems, RWTH Aachen University, 52074 Aachen, Germany
[2]ICE-1: Energy Systems Engineering, Forschungszentrum Jülich, 52425 Jülich, Germany
[3]Eaton Research Laboratories (ERL), 52074 Aachen, Germany
[4]HESSTec, 46980 Valencia, Spain
[5]INESC TEC, 4200-465 Porto, Portugal
[6]JARA-Energy, 52425 Jülich, Germany
[7]Fraunhofer FIT, Center for Digital Energy, 52068 Aachen, Germany

Corresponding author: Chandra Sekhar Charan Dande (charan.dande@eonerc.rwth-aachen.de)

This work was supported in part by European Commission Horizon Europe Programme under Grant Agreement 101096511 and in part by InterSTORE.

ABSTRACT Interoperability among diverse devices, from traditional substation control rooms to modern inverters managing components like Distributed Energy Resources (DERs), is a primary challenge in modern power systems. It is essential for streamlining decision-making and control processes through effective communication, ultimately enhancing energy management efficiency. This paper introduces the open-source Legacy Protocol Converter (LPC) grounded in the IEEE 2030.5 standard, which incorporates advanced features for improved adaptability. The LPC bridges legacy equipment using standard protocols such as Message Queuing Telemetry Transport (MQTT) and Modbus with a light-weight asynchronous Neural Autonomic Transport System (NATS) communication system. In light of the limitations inherent in traditional synchronous RESTful systems—specifically those compliant with IEEE 2030.5 that are incapable of facilitating multiple endpoints—the adoption of asynchronous NATS is implemented. This approach can notably enhance communication flexibility and performance. The implementation is containerized for efficient service orchestration and supports the reusability of solutions. The LPC is engineered for seamless integration of DERs with Energy Management System (EMS), aggregation platforms, and Hardware-in-the-loop (HIL) testing environments. In this paper, the LPC has been tested and further developed in various use cases such as multi-physics optimization involving HIL and fast frequency services, e.g., virtual inertia and load shedding, each in a different architectural setup. The findings validate the applicability of LPC not only for devices within modern power systems, but also for heat pumps in the thermal energy sector, facilitating sector coupling. Moreover, the paper provides additional insights into LPC's functionality, reaffirming its efficacy as a scalable, robust, and user-friendly solution for bridging legacy systems through the enhanced IEEE 2030.5 standard designed for the monitoring and control of DERs.

INDEX TERMS IEEE 2030.5, interoperability, legacy protocol converter, load shedding, multi physics optimization, neural autonomic transport system, virtual inertia.

I. INTRODUCTION

Within the context of the electricity grid, there is a notable increase in the penetration of Distributed Energy Resources (DERs), which is attributed to an enhanced awareness of

The associate editor coordinating the review of this manuscript and approving it for publication was Jose Saldana.

decarbonization [1]. These DERs include generations such as rooftop Photovoltaic (PV)s, extending to storage solutions like Battery Energy Storage System (BESS), and including controllable loads such as Electric Vehicle (EV)s and Heat Pump (HP)s. Nonetheless, each technological advancement is accompanied by its own array of vendor diversity; as reported in [2], a single automotive manufacturer offered a total of 29 fully electric vehicle models by the year 2023, each model exhibiting unique charging characteristics, energy storage capacities, and control interfaces. In another instance, grid-forming inverters from one manufacturer present diverse firmware and communication interfaces [3]. These examples underscore the growing heterogeneity among DERs, even when originating from a single manufacturer, and emphasize the diversity of various assets in modern power systems. This lack of a unified and standardized approach results in increased costs, inefficiencies, and heightened cybersecurity vulnerabilities. Hence, interoperability, i.e., seamless communication and integration among varied systems, devices, and applications, is essential for the synchronization of operations across diverse DERs and the achievement of unified energy management objectives.

According to the CEN-CENELECC-ETSI Smart Grid Coordination Group (SG-CG) [4], interoperability is defined as "*the ability of two or more networks, devices, systems, applications, or components to interwork, exchange and use information in order to perform required functions*". Ensuring interoperability facilitates different entities within the smart grid, including DERs from a multitude of manufacturers, to communicate and share information. This interoperability offers distinct advantages to various stakeholders. For instance, the Transmission System Operators (TSOs) can enhance grid stability and reliability of the network through remote access of various DERs within the system [5]. From the consumer perspective, there is increased flexibility in demand management, allowing the automation of demand shifts from peak to off-peak periods. In addition, optimal utilization of electrical infrastructure is achieved by postponing the need for grid modifications, likely leading to a reduction in operational costs imparted to consumers. From a business perspective, interoperability mitigates proprietary restrictions associated with vendor-controlled devices protected by trade-protected patents, thereby expanding market access.

In a smart grid, interoperability can be achieved through the IEEE 2030.5-2018 protocol, a communication standard with strong security requirements, such as encryption and authentication, that prevent cyber-attacks [6]. Many current DERs and grid components rely on proprietary or outdated communication protocols, creating compatibility issues when interfacing with advanced smart grid infrastructure [7]. Integrating legacy systems and existing communication protocols with modern communication standards poses a significant challenge. Owing to a lack of a unified and standardized approach, protocol converters are essential to bridge this gap by enabling seamless data exchange between legacy systems and IEEE 2030.5-compliant platforms.

The importance of communication gateways to facilitate the interoperability among protocols has been highlighted in [8]. The authors of [9] present an open information architecture for the integration of DERs, in which the interoperability between communication protocols is addressed through a connectivity module containing communication adapters that handle the protocol conversion. Nevertheless, the implementation did not incorporate a publisher/subscriber messaging system. The utilization of such a system would enable the decoupling of physical, network, and logical layers. Moreover, the integration of a publisher/subscriber messaging framework would provide independence from specific programming languages, operating systems, and physical communication media, such as Wi-Fi and cellular networks. An open-source framework for validating DERs interoperability is presented in [10], including a Modbus to IEEE 2030.5 protocol converter. However, it was assumed that the DERs must communicate in either Modbus, IEEE 2030.5, or IEEE 1815, which is not always the case in legacy systems. Furthermore, neither the connectivity module presented in [9], nor the protocol converted presented in [10] are publicly available. An open-source platform for sensing and control applications is presented in [11], namely Eclipse VOLTRRON. This platform allows applications like intelligent load and transactive energy control, and can be integrated with software tools like Matlab and standards like OpenFMB [12], [13]. Despite the availability of numerous existing studies and related open-source tools, IEEE 2030.5 has predominantly been utilized solely as a behind-the-meter protocol. IEEE 2030.5, if utilized in the entire architectural framework, enables coherent communication from customer DERs to aggregators to distribution system operators (DSOs) and TSOs. Furthermore, it supports real-time situational awareness and coordinated control for grid stability and flexibility services. Notably, other research endeavors, such as [12], acknowledge the significance of employing publish/subscribe-based messaging systems, such as the NATS protocol, for facilitating peer-to-peer communication among utility devices at a conceptual level; however, these have not been integrated into practical implementations. To the best of the authors' knowledge, there are no existing open-source protocol converters that facilitate communication using IEEE 2030.5 throughout the entire architectural framework, while concurrently incorporating a publish/subscribe messaging client, specifically the NATS protocol.

In a previous work [14], we introduced the Legacy Protocol Converter (LPC) a open source protocol converter, facilitating communication using IEEE 2030.5 throughout the entire architectural framework with NATS as a publish/subscribe messaging client. The LPC is designed to enhance interoperability between legacy energy systems and modern smart grid communication standards based on IEEE

2030.5. Furthermore, [14] introduces the use of LPC in different architectures and illustrates the LPC deployment in the use case of fast peak shaving utilizing a particular architecture. This paper elucidates the LPC deployment in all the proposed architectures across diverse use cases such as multi-physics optimization involving Hardware-in-the-Loop (HIL) and fast frequency services. These different use cases showcase the practical implementation of the LPC in a variety of scenarios commonly arising from the integration of DERs, and Hybrid Energy Storage System (HESS), in power systems. Furthermore, the paper provides insights into the LPC implementation, such as configuration files developed, resource utilization in hardware, and software servers. Moreover, the difficulties encountered during the execution of the LPC and implementation of interoperability, particularly in relation to IEEE 2030.5, are meticulously outlined, accompanied by the provision of the corresponding remedial strategies. The LPC supports standard protocols including Modbus and Message Queuing Telemetry Transport (MQTT), while utilizing asynchronous communication via Neural Autonomic Transport System (NATS). This enhances flexibility and performance compared to conventional synchronous REST APIs, which constitute the predominant communication approach for IEEE 2030.5 in existing state-of-the-art protocol converters. By integrating containerization technologies (such as Docker Compose) for service coordination, a scalable and user-friendly solution is delivered, facilitating the seamless transition of legacy systems to an IEEE 2030.5-based enhanced monitoring and control framework.

The main contributions of this paper are as follows:

1) a detailed explanation of the LPC and its internal components;
2) effectiveness of the LPC as an interoperability tool is validated in various use cases that commonly arise from the integration of DERs, namely multiphysics optimization, virtual inertia and load shedding;
3) insights into the LPC implementation are presented alongside a discussion of the challenges faced during the LPC execution and the corresponding solutions applied.

The subsequent sections of this paper are structured as follows: Section II introduces the interoperability framework within the InterSTORE project, elucidating the context for standardized communication in modern energy systems. Section III elucidates LPC, detailing its internal architecture and deployment. Section IV details the deployment of LPC for the use case of multi-physics optimization involving HIL through a ''Dual Cascaded LPC Architecture''. Section V details the deployment of LPC for the use case of Virtual Inertia through a ''Single LPC Architecture''. Section VI details the deployment of LPC for the use case of Islanding and Load Shedding through ''LPC cascaded with Another Protocol Converter Architecture''. Furthermore, Section VII provides a comprehensive analysis of the insights and challenges (along with their solutions) associated with LPC's functionalities. Finally, Section VIII provides the conclusions, summarizing key findings and outlining future research directions.

II. INTEROPERABILITY

There are different approaches to interoperability, which can co-exist and can be categorized into two groups: ontology-based and dictionary-based. An ontology-based approach comprises a vocabulary of terms and specifications, which includes definitions and indications of how concepts are interrelated [15]. In the energy domain, popular ontologies are Smart Applications REFerence (SAREF), Ontology of unit of Measure (OM), or Open Energy Ontology (OEO). Furthermore, the ontology based approach allows for inferences or reasoning between terms (relationships) and is a powerful way to interoperate [16], [17], and [18]. It can, however, be time-consuming and difficult to implement when the configuration file becomes large. A dictionary-based approach entails the utilization of a predefined corpus of information accompanied by an explicitly articulated and well-defined set of operational rules [19]. Some well-known dictionary approaches are Open Automated Demand Response (OpenADR), a data model for an automatic demand response [20], and IEEE 2030.5, which is a data model standard for smart grid [21].

To achieve interoperability in a large-scale DERs system, it is imperative that the architecture meets several essential criteria, including a comprehensive data model, scalability, flexibility, and robust cybersecurity measures. Firstly, a comprehensive and standardized data model is essential for the integration of a diverse range of DERs. It acts as syntactic interoperability, ensuring that data exchanged between systems is structured in a standardized format. Without syntactic interoperability, systems struggle to interpret and process data correctly, leading to inefficiencies and miscommunication. If the architecture is designed to be scalable, it will be capable of maintaining functionality even as the number of clients increases substantially. Moreover, a flexible setup will enable users to support multiple deployments within the same architectural framework. Lastly, cybersecurity is of paramount importance in the context of the smart grid. Despite the presence of various encryption and certification measures, the incorporation of proxies and masking into the architecture remains a critical requirement.

Considering the above requirements, IEEE 2030.5 is chosen as a data model and NATS as a communication system. IEEE 2030.5, which is formerly known as SEP 2.0, is a communication protocol developed to support smart grid operations, essentially for DERs integration [6]. Currently, protocols like IEC 61850 are used for the control of grid-assets such as circuit breakers, however, there is a need to communicate with consumer-owned assets such as DERs and smart meters. IEEE 2030.5 can cover this gap to achieve complete smart grid interoperability. Moreover, IEEE 2030.5 not only facilitates syntactic interoperability

but also ensures semantic interoperability, thereby aiding in the integration of devices that operate using proprietary protocols from various vendors [14]. NATS, occasionally referred to as message-oriented middleware, is an open-source messaging system [22]. The fundamental features of NATS are scalability, performance, and ease of use. As NATS enables many-to-many communication, multiple Energy Management System (EMS) can interact with various devices, thereby supporting geographically distributed DERs. Additionally, the incorporation of NATS as a middleware effectively decouples DERs from the EMS. As a result of EMS's independence, DERs can be integrated seamlessly without necessitating any modifications to the EMS. Furthermore, a layer of abstraction using NATS also mitigates the risks associated with cyber security attacks such as denial of service (DOS) and distributed DOS [14].

III. LEGACY PROTOCOL CONVERTER (LPC)

The LPC [23] is an open-source, lightweight, and modular software tool developed within the framework of the InterSTORE European Union (EU) project [24]. Its primary objective is to enable interoperability between legacy assets based on Modbus, and MQTT-such as PV systems, BESS, and EMS-and modern platforms based on IEEE 2030.5. The LPC addresses a widespread challenge in the energy domain, where legacy systems remain prevalent across residential, commercial, and industrial installations, yet lack native support for emerging communication standards.

The tool was initially developed by Sunesis, ~~a project partner~~, and has since evolved into a community-maintained project. It is currently deployed in different pilot sites, for demonstration purposes. In Austria, where in the context of an energy community, Modbus-based assets from 20 households are integrated into the cloud-based EMS CyberNoc, to optimize the energy consumptions of the overall community. In Germany, at the Living Lab Energy Campus (LLEC) of Forschungszentrum Jülich (FZJ), where a diverse set of commercial DERs assets are integrated within the campus environment and managed via the FIWARE-based Information and Communication Technology (ICT) platform [25], [26]. In Portugal, where various BESS, including second-life batteries, have been integrated into the EMS of a parking lot for EV to smooth the consumption peaks and improve node flexibility. In Italy, at Rome Enel X's XLab, with the end-to-end integration of diverse assets—including PV, BESSs, and Vehicle-to-Grid (V2G) EV chargers—into a flexibility market framework including a dual-flow implementation for telemetry and control, enabling real-time flexibility services. In Spain, at Hybrid Energy Storage Solutions SL (HESStec)'s Advanced Grid Lab, where the LPC was used to validate the fast-response services such as successful execution of black start, voltage dip, and Automatic Transfer Switch (ATS) scenarios using grid-forming and grid-following DERs operating under real-world conditions [27], [28].

A. ARCHITECTURE AND DEPLOYMENT

The LPC is designed as a middleware translator that ensures secure, real-time communication between heterogeneous components. It is capable of running on minimal hardware, such as Raspberry Pi (RPi) Single-Board Computer (SBC), facilitating edge deployments without requiring firmware modifications to legacy equipment. This makes it suitable for scalable deployments, ranging from small residential sites to complex industrial infrastructures.

The LPC consists of two main configurable blocks:

- Connections: define the communication endpoints, e.g., EMS or DERs units, specifying the necessary parameters such as host, port, protocol type (MQTT, Modbus TCP/Remote Terminal Unit (RTU), or IEEE 2030.5), security credentials (username/password, SSL), and protocol-specific settings (e.g., baud rate, parity for Modbus RTU).
- Transformations: define the data translation logic between protocols. Each transformation maps messages from source to destination, specifying input/output topics, message formats, and data structures.

This modular design allows the LPC to support multiple concurrent connections, translating data between endpoints with low-latency performance. For instance, telemetry data received via Modbus can be reformatted and published to an MQTT broker with topic-specific routing, or ingested into an IEEE 2030.5-compliant EMS.

B. MESSAGE MAPPING AND TRANSFORMATION

The core of LPC's translation logic resides in its flexible message transformation engine, configured via YAML files.

This file contains two main components: `connections` and `transformations`, the latter being central to message handling.

1) TRANSFORMATION STRUCTURE

Each transformation block within the configuration defines a complete translation workflow from one or more input protocols to one or more output formats. A transformation consists of the following nested subfields:

- **General**: Contains metadata such as `name` and `description`, allowing users to document the purpose of the transformation.
- **Connections**: Specifies the list of input and output connections (e.g., MQTT topics, Modbus registers, IEEE 2030.5 services) involved in the transformation. Each connection entry defines parameters such as:
  - Protocol type (e.g., MQTT, Modbus TCP/RTU, Hypertext Transfer Protocol (HTTP));
  - Topic or register to listen to (for incoming connections) or publish to (for outgoing connections);
  - Data format (e.g., JSON, binary, structured payload).
- **Message**: Defines the message template and transformation logic. The message section uses key-value pairs to

describe how data is extracted, transformed, and inserted into the outgoing format.

2) MAPPER CONFIGURATION

Within the `message` block, *mappers* are used to define the transformation logic at a granular level. Each field in the outgoing message can be constructed using a mapper, which supports the following parameters:

- **type**: specifies the target data type (e.g., `integer`, `float`, `string`, `datetime`);
- **path**: indicates the JSON path or register index in the input message from which to extract the value;
- **pattern**: required when converting time or date values; defines the format string for parsing or formatting datetime values (e.g., `yyyy-MM-dd'T'HH:mm:ssZ`);
- **values**: provides a static list of enumerated mappings, useful for encoding or decoding categorical values;
- **default** (optional): specifies a fallback value if the input field is missing or invalid.

This fine-grained control allows users to perform not only simple one-to-one field mappings and formatting messages for compliance with standard schemas like IEEE 2030.5, but also type conversions, value translations, and structural reorganization of message payloads.

3) BENEFITS AND FLEXIBILITY

This declarative configuration model enables rapid integration of new devices and systems without code changes, making the LPC adaptable to evolving project requirements. It allows engineers to map data flows intuitively, reducing development and maintenance effort while ensuring data consistency and protocol compliance. The LPC provides an intuitive web-based interface [29] for configuring protocol mappings, streamlining setup even for users without deep technical expertise. Additional optional features include:

- Logging: Customizable logging for diagnostics and performance monitoring.
- Registration: Support for automatic registration of LPC instances to external systems via MQTT or HTTP endpoints.
- Security: Integration of encryption and authentication mechanisms to safeguard data exchange and prevent unauthorized access.

In summary, the LPC's message transformation capabilities provide a powerful and flexible foundation for interoperability across legacy and modern systems, supporting not just protocol translation but also semantic alignment and structural adaptation of messages.

C. ROLE IN THE FUTURE EMS ARCHITECTURE

The LPC is aligned with emerging trends in microservice-based EMS, where communication is increasingly topic-oriented and broker-mediated (e.g., via MQTT) [30], [31]. In such architectures, the LPC serves as a protocol bridge, ensuring that data from legacy systems can be dynamically routed to modern EMS services and cloud-based analytics platforms.

(a) BESS 1 (b) BESS 2 (c) Photovoltaics (PV) (d) Heat Pumps (HP)

FIGURE 1. Overview of DERs integrated in the MPES at FZJ.

By enabling protocol-agnostic communication, the LPC contributes to extending the operational lifespan of legacy infrastructure, promoting digital integration, and reducing overall upgrade costs. The following section demonstrates LPC deployments in real-world settings, validating its adaptability, reliability, and performance in diverse environments.

IV. MULTI-PHYSICS OPTIMIZATION

One of the use cases enabled by the LPC is about the coordinated control of DERs within a Multi-Physics Energy System (MPES) behind-the-meter of an energy consumer. The concept of ''multi-physics'' stems from the integration of DERs, particularly electric HPs, which link the thermal and electrical energy sectors. As the transition to a low-carbon energy system accelerates, systems that leverage interactions between different energy carriers are gaining prominence [32]. HPs, in particular, offer a highly efficient and flexible solution for low-emission heating. They contribute to reducing greenhouse gas emissions and enable responsive energy management, thereby improving the sustainability and performance of energy systems.

An effective EMS is required for MPES to support the reliable and sustainable operation of such complex, integrated energy systems. While multiple architectures, control timelines, and algorithmic approaches can be designed to fulfill these criteria, Appendix A introduces the specific concept implemented on the FZJ campus as part of the InterSTORE project demonstrations. In Figure 1, the DERs integrated in the MPES of FZJ via the presented MPES concept are shown.

To implement the proposed Energy Management (EM) concept, several functional requirements must be fulfilled. Firstly, an EM platform is required to host and execute the control algorithm in real-time. This platform must also

FIGURE 2. Eaton SMP 4250 deployed at FZJ.

be capable of storing essential metadata—such as battery capacity and the power range of the HP—which reflect the physical characteristics of the MPES. Secondly, bidirectional communication with DERs is required, as the algorithm depends on real-time data inputs from Behind the Meter (BTM) assets—formally represented by P_L, P_G, S_h, and S_b in the pseudocode presented in Appendix A—and generates control outputs (p_h and p_b) that must be communicated back to the respective devices. In the FZJ demonstration, the Eaton Substation Automation Platform (SMP 4250, depicted in Fig. 2) was used to host the algorithm [33], which was implemented using the CODESYS programming environment. The second functional requirement, real-time communication, was enabled through the interoperability concept facilitated by the LPC.

In the setup considered, there are batteries, loads, and generators that communicate via Modbus, HPs use MQTT, and SMP 4250 platform that supports smart grid protocols such as DNP3, IEC 104, Modbus, and REST API. While the IEEE 2030.5 standard provides a structured messaging format and the LPC enables access to the NATS network using this structure, the targeted communication setup presented a challenge for direct LPC integration: neither the DERs nor the EMS natively support IEEE 2030.5. However, the lightweight and modular nature of the LPC can help system engineers overcome this problem with minimal effort. A practical solution involves cascading two instances of LPC in the communication chain, enabling protocol translation and semantic alignment between the DERs and the EMS. This approach, named as "Dual Cascaded LPC Architecture", illustrated in Figure 3, establishes an interoperability layer where the transmitted data follows IEEE 2030.5 standard models and all communications take place in NATS network without requiring native support of the endpoints for the standard.

In Fig. 4, the dashboard used to monitor the BESS 1 integrated in the MPES at FZJ is shown. The figure shows how the BESS is controlled (Test = 1) to inject 100 kW of active power into the system. The control setpoint sent to the BESS is shown as the yellow curve in the top graph, and the

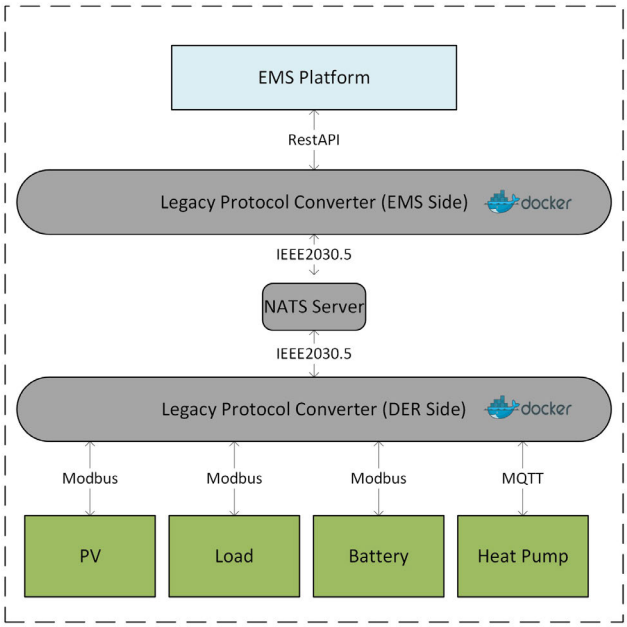

FIGURE 3. Dual LPC architecture to enable MPES in FZJ campus.

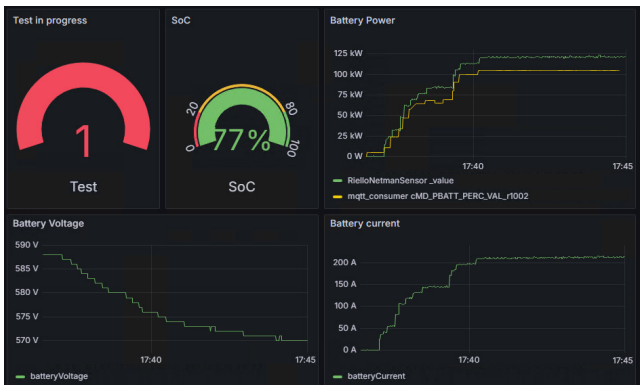

FIGURE 4. Dashboard of the BESS 1 integrated in the MPES at FZJ.

actual power drawn from the DC side of the BESS is shown as the green curve in the same graph. The difference between the two is due to the conversion losses and internal consumption of the system. It is worth noting that sensitive information regarding topics, IDs, and the like, has been covered for safety reasons.

Figure 5 shows the dashboard used to monitor the BESS 2 integrated into the MPES. In this case, the BESS is also being used to inject 8 kW of active power and 0 kvar of reactive power. As this is a different BESS, the controls are enabled by setting the dedicated control registers to values of 3 and 1 for active and reactive power, respectively. In the figure, the total active, apparent, and reactive powers injected by the BESS are shown in the top graph, while the active power monitored in the three phases at the Point of Common Coupling (PCC) is shown in the bottom graph.

The BESSs employed are sourced from different manufacturers. As can be seen in Figures 4 and 5 it is evident that the

FIGURE 5. Dashboard of the BESS 2 integrated in the MPES at FZJ.

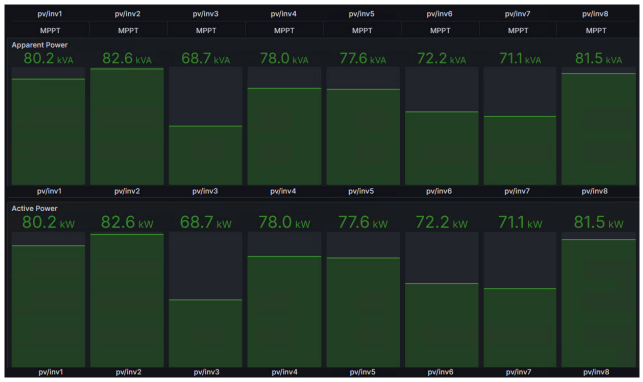

FIGURE 6. Dashboard of the PV integrated in the MPES at FZJ.

injected power exhibits a positive value in one system and a negative value in the other. This discrepancy arises from the fact that the manufacturers implement Modbus registers differently: one considers power drawn from the battery as positive, while the other considers power injected as positive, with opposite sign conventions being followed.

Figure 6 shows the dashboard displaying the status and power generated by each inverter in the PV field integrated into the MPES. It can be seen from the figure that all 8 inverters are operating in MPPT mode, while shadowing effects caused by clouds passing over the system are leading to differences in the power generated by each inverter.

Finally, Fig. 7 shows the dashboard used to monitor the HP system, including its thermal storage. The figure shows a phase in the early morning, during which the HP is used to heat the fluid going to the building with a heat flux of 439 W and an active power consumption of 387 W. During this phase, the thermal storage has an State-of-Charge (SoC) of 32.4%. However, due to the low heat demand and the corresponding low power consumption of the HP, the thermal storage is not currently in use.

V. VIRTUAL INTERTIA

In this section, the proposed LPC solution is employed in handling a fast frequency service called virtual inertia. Traditionally, the inertial response of power systems originated mainly from the inherent electromechanical behavior

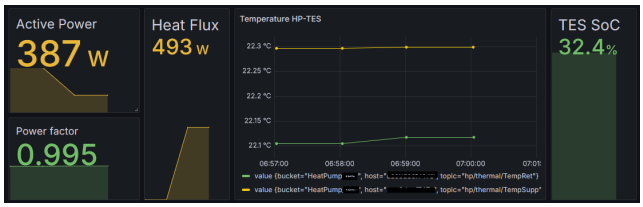

FIGURE 7. Dashboard of the HP integrated in the MPES at FZJ.

of synchronously rotating machines reacting to power imbalances. However, as these synchronous generators are increasingly being decommissioned or replaced by inverter-based resources (IBRs), there is a growing need to replicate this rotational inertia through control strategies implemented in IBRs. This substitute response must be inherent to the system, sufficiently robust, and proportionate to the magnitude of a disturbance in order to effectively reduce the Rate of Change of Frequency (RoCoF) and maintain system stability [34]. This type of control mechanism is commonly referred to as "Synthetic Inertia" [35]. In industry literature, similar concepts are also described under various terms, including "Active Inertia Power" [36], "Positive/Negative Inertia Power" [37], "Inertial Response" [38], and "Virtual Inertia Emulation (VIE)" [39]. The distinguishing feature of virtual or synthetic inertial responses is their rapid reaction to power disturbances, typically within 5 milliseconds, and their effect may last for several seconds. The synthetic inertial response involves a sharp active power injection in response to the RoCoF observed in the system.

The considered setup, as illustrated in Figure 8, consists of HESS, which includes a battery and an ultracapacitor (UCAPS) along with a Grid-Forming (GFM) converter. Furthermore, there is EMS for controlling the HESS and emulators that represent the grid and renewable energy sources. In this scenario, LPC is integrated through "Single LPC Architecture", as shown in Figure 9. The LPC is deployed within the device's local network using a virtual machine that hosts two Docker containers: one for the LPC and another for a local NATS message queue server. This setup allows the LPC to efficiently manage data transformations in both directions, enabling the EMS to read real-time data from the inverter (e.g., active power) and send control setpoints (e.g., power targets) to the inverter. Speed tests were conducted to evaluate the "Single LPC Architecture" by measuring the delays under varying conditions of CPU usage, polling rates, and number of data points. These tests confirmed the architecture's ability to handle real-time data exchange with minimal latency, an essential requirement for fast power services.

The virtual inertia algorithm is elaborated in Appendix B. Subsequently, the response of a HESS containing battery and ultracapacitor with virtual inertia algorithm against a step load change in the grid using different communication protocols, specifically, the proposed LPC solution and controller area network (CAN) approach. Figure 10 presents

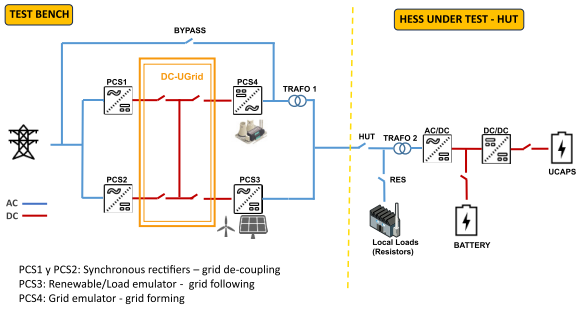

FIGURE 8. Grid laboratory scheme.

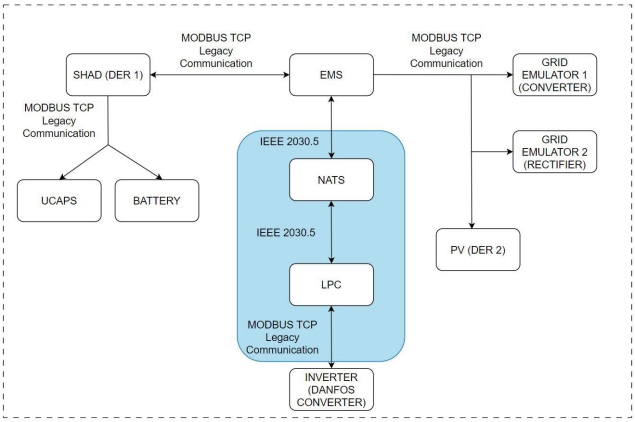

FIGURE 9. Single LPC architecture for virtual inertia in HESSTec gridlab.

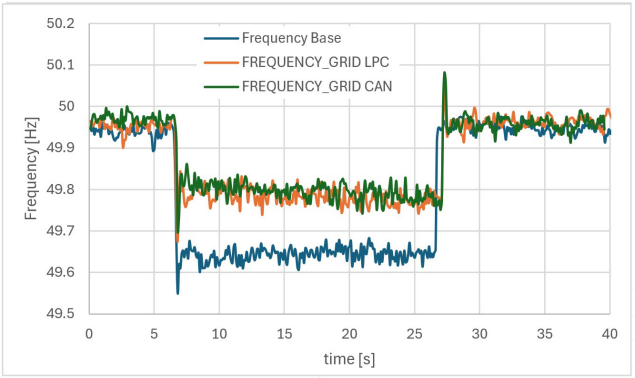

FIGURE 10. Frequency response against load step.

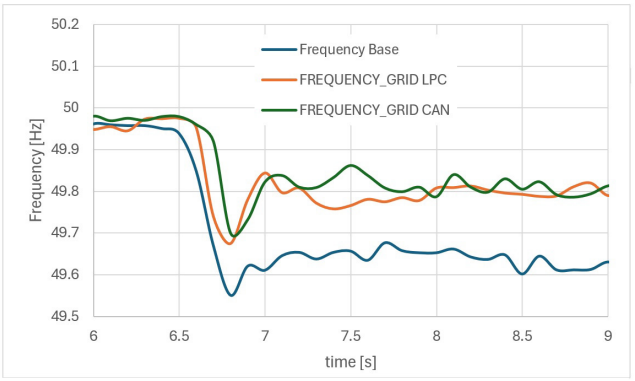

FIGURE 11. Frequency response against load step (zoom).

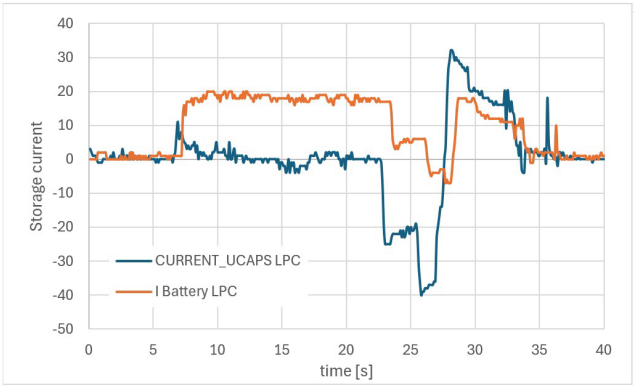

FIGURE 12. UCAP and battery current performance with LPC.

the frequency response to the introduction of a load step occurring at 6.5 seconds. It illustrates three distinct scenarios: the base scenario, characterized by the absence of HESS, and two additional scenarios in which virtual inertia is provided by HESS, utilizing both the CAN and LPC approaches, respectively. Figure 11 illustrates the magnified image of the said frequency response.

Figure 12 showcases the currents in UCAPS and battery through LPC. It can be observed that LPC was able to function in an environment that had storage systems with different behaviors. Table 1 details the comparison of the LPC and the CAN with respect to RoCoF and Nadir values. It can be seen that the LPC approach has a performance similar to that of the CAN approach.

VI. ISLANDING AND LOAD SHEDDING

A Software in the Loop (SIL) setup has been considered for evaluating the load shedding use case. This setup comprises a real-time simulator incorporating a practical model of a low-voltage microgrid operating on the RTDS platform, alongside a custom Python script running on the EMS, which computes and sends commands to various microgrid components. The low-voltage microgrid employed is a slightly modified version of the Banshee microgrid. This adjustable small-scale industrial setup is backed by three utility radial feeders [40]. The feeders have a limited connectivity through switches, each eligible to carry its critical load. The total electricity demand varies from 5 MW to 14 MW for the minimum and maximum loads. The system ratings include medium voltages of 4.16 kV and 13.8 kV, and low voltages of 208 V and 480 V. There are around 18 aggregated loads supplied by the feeders. The list of various components is enumerated in Appendix C. In this study, the load shedding use case is implemented to evaluate one of the rapid frequency services that can be delivered by the proposed LPC.

TABLE 1. RoCoF and Nadir in different cases.

Case	RoCoF (Hz/s)	Nadir (Hz)
Event	1.33	49.55
CAN	0.9	49.7
LPC	1	49.68

Additionally, through this use case implementation, the effectiveness of LPC in translating between MQTT and IEEE 2030.5 has been demonstrated. Figure 13 shows a simplified schematic of this setup, called as LPC cascaded with Another Protocol Converter Architecture. To this end, the GTNET card of the RTDS real-time simulation platform is used. Since this card doesn't support MQTT directly, the VILLASnode [41] gateway was used as an intermediate module to get UDP packets from GTNET and convert them to MQTT, and encode the payload in JSON format. Here, it was beneficial to set up a containerized solution, taking advantage of the existing VILLASnode and LPC Docker containers, as well as well-known containers for Python and the two required message brokers, namely Mosquitto for MQTT and the official NATS container. The flexibility of VILLASnode allows extending this scenario to a Geographically-Distributed Hardware-in-the-loop (GD-HIL) setup, where multiple stakeholders can participate without compromising their intellectual property [42]. Moreover, the MQTT payload provided by VILLASnode follows the message format shown in code listing VI. The payload consists of a timestamp element, namely `t_s`, in which the `t_s` element specifies the number of seconds and milliseconds. The `sequence` corresponds to the received packet's sequence number. Finally, the `data` field is a vector with the signals comprising this specific sample. Note that in this payload, the signals are organized based on their position in this field. For instance, the first element in code listing VI is the system frequency, whereas the second element is the voltage of a bus in p.u.

Initially, dynamics are introduced to the grid by transitioning a specific region of the grid into Islanding mode. Subsequently, the pertinent circuit breaker of the feeder is tripped, resulting in a decline in the frequency of the area. Upon the frequency reaching the lower threshold of 49.5 Hz, the load shedding algorithm is activated, subsequently disconnecting the largest load in the region, thereby restoring the frequency to within acceptable limits. The formulation of the workflow is elaborated in Appendix C. Figure 14 showcases the plot of frequency, where at *(1)* a section of the grid enters islanding mode, and at *(2)* the frequency falls below 49.8 Hz, thereby triggering the load shedding algorithm. The frequency is back to nominal value (shown as *(3)*) in 333 ms.

VII. INSIGHTS OF LPC IMPLEMENTATION AND FUNCTIONALITIES

In the previous sections, the LPC is deployed in various use cases, each with its own set of conditions and challenges.

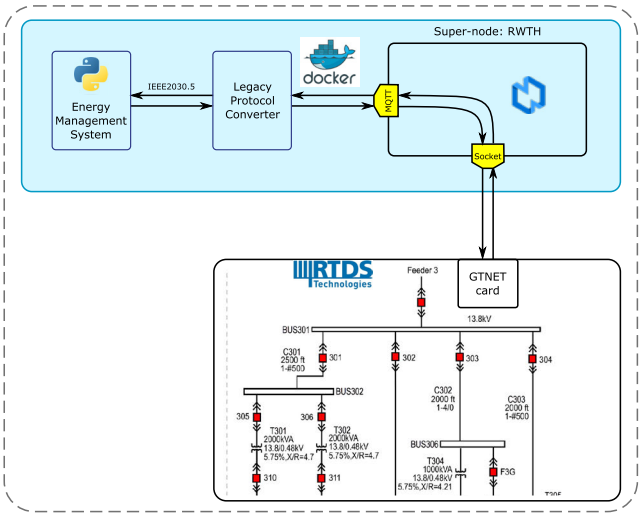

FIGURE 13. LPC cascaded with another protocol converter architecture for load shedding.

```
[
    {
        "ts": {
            "origin": [
                1717487454,
                334867570
            ]
        },
        "sequence": 814,
        "data": [
            50.000003814697266,
            0.059899438172578812
        ]
    }
]
```

Listing 1. Example VILLASnode JSON payload.

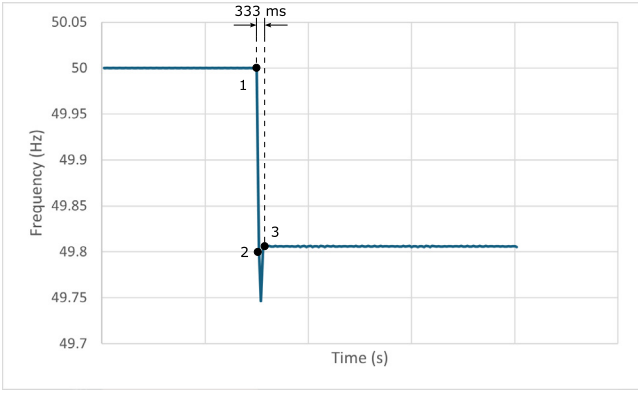

FIGURE 14. Islanding and Load Shedding in the banshee microgrid ruuning in the realtime simulator RTDS.

In MPES, the LPC is integrated in the presence of both electrical and thermal components. In the use case of virtual inertia, the grid undergoes rapid power fluctuations that needs to be compensated by a sharp active power injection. In the use case of islanding and load shedding,

the SIL setup has been considered, where the LPC was cascaded with another protocol converter. Throughout the implementation phase, various challenges were encountered specific to each use case, leading to enhancements in the LPC. These improvements are elucidated in this section. Furthermore, insights are provided into the implementation of the LPC, with particular emphasis on computational cost and the challenges faced in deploying the LPC within the mentioned use cases.

In the setup of MPES, the SMP 4250 platform supports smart grid protocols such as DNP3, IEC 104, Modbus, and REST API; the DERs themselves use heterogeneous protocols (i.e., batteries, loads, and generators communicate via Modbus whereas HPs use MQTT). Moreover, the DERs operate under different native communication architectures: battery and load meters act as Modbus servers in a conventional client-server setup, where the EMS determines the polling frequency; in contrast, HP push their status updates via MQTT, with the event initiated on the device side. This heterogeneity introduces a synchronization challenge when consolidating real-time data from all DERs. Without proper alignment, the EMS may process outdated or inconsistent input data, leading to suboptimal or even incorrect control decisions. The LPC features an important function that solves this issue, by harmonizing communication flows with the help of an external clock (e.g., NTP server) that determines MQTT publishing instances as well as Modbus reading instances. Using the IEEE 2030.5 data model, these time-stamped status data are incorporated in pertinent message types such as *DERStatus*. This approach allows mapping from MQTT messages and Modbus registers to NATS messages such that all DERs-to-EMS and EMS-DERs data exchanges are semantically consistent with a unified temporal reference.

Another significant challenge was due to the abstract nature of definitions within IEEE 2030.5 data models. As the array of devices expands to incorporate multi-energy technologies such as heat pumps and storage elements utilizing alternative energy carriers like thermal energy storage, specific data structures, such as *DERStatus.stateOfChargeStatus.value* becomes impractical for effectively representing pertinent data. Consequently, there is a reliance on less rigorously defined data models such as *MirrorMeteringList*. Nevertheless, the interpretation of these message formats necessitates that system developers implement custom logic on the EMS side, thereby constraining the convenience and straightforward utility of IEEE 2030.5 data models.

In the context of MPES, Table 2 outlines the number of configuration files required for the integration of each DERs, and the input and output protocols used for each transformation corresponding transformation, taking the flow of information from DERs to EMS (from bottom to top of Fig. 3) as a reference. In particular, transformation 1 is used to convert Modbus and MQTT messages to the interoperable standard IEEE 2030.5, while transformation 2 converts the associated quantities into MQTT, so that they can be read by the RestAPI of the EMS platform. This approach ensures an interoperable layer between the two LPC outlined in Fig. 3 where IEEE 2030.5-compliant messages can be exchanged simply by communicating with the NATS server.

TABLE 2. Configuration files developed for the MPES integration.

DER	Config Files	Transformation 1		Transformation 2	
	Number	Protocol in	Protocol out	Protocol in	Protocol out
BESS 1	7	Modbus	IEEE 2030.5	IEEE 2030.5	MQTT
BESS 2	2	Modbus	IEEE 2030.5	IEEE 2030.5	MQTT
PV	9	Modbus	IEEE 2030.5	IEEE 2030.5	MQTT
HP	1	MQTT	IEEE 2030.5	IEEE 2030.5	MQTT

TABLE 3. Resource usage on the RPi.

Container name	CPU usage		
	Min	Average	Max
LPC	9 %	25 %	47 %
NATS server	0.1 %	0.3 %	0.9 %

As outlined in the table, integrating BESS 1 required seven configuration files. This BESS comprises three inverters, each of which is monitored and controlled with a dedicated interface (thus two configuration files are needed for each interface), plus one configuration file to monitor voltages and powers at its PCC with the network via a dedicated power quality meter. BESS 2 is composed by a single inverter that utilizes a single interface for both monitoring and control (thus, 1 config file required). Also in this case, a power quality meter has been integrated to monitor electrical quantities at the PCC. The PV field is composed of 8 inverters, each with one interface for monitoring and control, thus requiring the integration via 8 different config files, plus one for the PCC monitoring. Finally, the integration of the HP required only one config file, since both thermal and electrical quantities of interest can be gathered via the same interface, using different MQTT topics.

The dual LPC architecture has been deployed on a RPi 4B with 8 GB of RAM to demonstrate that such a complex setup can be implemented on a low-cost SBC. Docker containers have been used to deploy both the LPC, hosting all 19 configurations, and the NATS server. In table 3, the minimum, average and maximum usage of CPU resources is reported for each container. It has to be noted that the config files of BESS 1, BESS 2, and PV are configured to gather Modbus messages every second from the DERs, while the HP config file collects data every minute, due to the larger reporting rate of the HP.

The results presented in the table demonstrate how the RPi can easily facilitate data exchange in such a complex scenario despite its limited computational capabilities. It is worth noting that higher CPU usage is observed, particularly by the LPC container, in the event of communication network issues

TABLE 4. Resource usage on a server.

Container name	CPU usage		
	Min	Average	Max
LPC	0.38 %	11.19 %	43.4 %
NATS server	0.05 %	0.11 %	0.20 %

not related to this demonstration setup (e.g., larger delays and packet loss due to an unusual load on the FZJ communication network). Similarly, an LPC Cascaded with Another Protocol Converter architecture, having one configuration file that transforms MQTT to IEEE 2030.5, is deployed on a Linux machine with 16 GB RAM, with LPC and NATS deployed in Docker containers. Table 4 details the minimum, average, and maximum usage of CPU resources is reported for each container.

VIII. CONCLUSION

This paper presents the LPC as a viable solution for interoperability in accordance with the IEEE 2030.5 standard. The study illustrates three distinct use cases where the LPC is implemented across three architectural configurations. Specifically, in the domain of multi-physics optimization, LPC is employed in a Dual Cascaded Architecture within a multi-energy landscape incorporating batteries and heat pumps, thereby facilitating sector coupling. Furthermore, in the MPES setup, due to different protocols, there was a challenge of heterogeneous communication flow; this was solved with the help of an external clock. In the context of Virtual Inertia, LPC is utilized within a Single LPC architecture to deliver fast frequency services, demonstrating its applicability in modern frequency management. Notably, the LPC was able to accommodate the sharp active power injection required for the use case of virtual inertia. In the scenario concerning load shedding, the LPC is integrated with an additional protocol converter to deliver standardized grid services such as islanding and load shedding. It is evident that the LPC possesses the versatility to function as a single protocol converter or in conjunction with another protocol converter. However, while integrating multiple protocols via the LPC, there was a challenge of temporal synchronization, which was solved by adding time-stamped status data in the messages of the IEEE 2030.5 data model. The scenarios presented in Sections V and VI, wherein frequency deviations are mitigated, illustrate that the entire process—which encompasses the detection of frequency deviations, the transmission of control signals, and the ensuing stabilization—transpires within a timeframe of less than one minute. This duration is well within the permissible timescale for primary frequency control. With regard to the IEEE 2030.5 data model, with devices expanding to other sectors such as thermal energy, specific structures need to be incorporated into the data model. Overall, it was demonstrated that the LPC effectively operates with hardware-in-the-loop systems from various energy sectors, expanding its capabilities from providing rapid frequency services to standard grid services.

APPENDIX A
ENERGY MANAGEMENT ALGORITHM FOR MULTI PHYSICS OPTIMIZATION

This EMS concept is characterized by its simplicity, responsiveness, and alignment with overarching system goals. It relies on linear analytical tasks, including a rule-based control algorithm that avoids complex non-linear optimization, thereby enabling fast and efficient real-time operation. The algorithm continuously analyzes the system state and computes set-points for DERs over short control intervals (e.g., 5 minutes), ensuring adaptability to dynamic conditions. Additionally, it operates based on high-level reference parameters—such as target SoC levels for both battery and thermal storage—which are determined in advance to reflect broader system objectives. These references guide the local control actions, ensuring coherence between real-time decisions and long-term energy management goals. The algorithm that determines these decisions was built considering the following boundary conditions:

- **Constant Coefficient of Performance (COP) over control horizon:** The COP of the HP is assumed to remain constant during each control interval (e.g., 5 minutes), enabled by stable temperatures on both the heat source, i.e., Low Temperature District Heating (LTDH), and sink, i.e., Thermal Energy Storage (TES) sides.
- **Thermal comfort ensured via TES:** Building thermal comfort is maintained as long as the TES retains a sufficient SoC, since the HP indirectly contributes to heating by charging the TES.
- **Predefined TES SoC reference:** An a priori process—executed by either the BTM EMS or an external entity—provides a minimum SoC reference for the TES, which determines whether the HP should operate during the next control interval.
- **Real-time system measurements:** The algorithm relies on accurate real-time data for PV generation, electrical load, and SoC levels of both the battery and TES, communicated through the system architecture.

Based on these assumptions, the algorithm is designed to reduce the power exchanged with the main grid while ensuring that thermal comfort within the building is maintained. The following section provides a formal description of the algorithm with its pseudo code (Algorithm 1), and Table 5 outlines the relevant parameters and control variables used in its implementation.

To determine the feasible operation ranges, the algorithm first calculates the upper bound of the HP's electrical power consumption $\overline{P_h}$ by estimating the thermal energy the TES can still store, dividing it by the control horizon ΔT, and converting it to electrical power using the COP η_h, while ensuring it does not exceed the HP's rated capacity (**Line 1**).

TABLE 5. List of parameters and control variables in MPES algorithm.

Symbol	Description	Type – Source
ΔT	Control horizon	Parameter – Selected a priori
E_h	Energy capacity of TES	Parameter – Device specification
E_b	Energy capacity of battery	Parameter – Device specification
η_b	Charge-/Discharge efficiency of battery	Parameter – Device specification
P_h^+	Maximum electrical power input to HP	Parameter – Device specification
P_b^+	Maximum charge power to battery	Parameter – Device specification
P_b^-	Maximum discharge power to battery	Parameter – Device specification
$\underline{S_h}$	TES SoC reference	Parameter – Calculated a priori
η_h	Coefficient of performance of HP	Parameter – Measured in real-time
S_h	SoC of TES	Parameter – Measured in real-time
S_b	SoC of battery	Parameter – Measured in real-time
P_L	Electrical loads	Parameter – Measured in real-time
P_G	PV generation	Parameter – Measured in real-time
p_h	Electrical power consumption of HP	Control variable
p_b	Electrical power consumption of battery	Control variable

Algorithm 1 Multi-Physics EMS Control Algorithm

1: $\overline{P_h} \leftarrow \min(E_h \cdot (1 - S_h \cdot \Delta T \cdot \eta_h), P_h^+)$
2: $\overline{P_b} \leftarrow \min(E_b \cdot (1 - S_b \cdot \Delta T), P_b^+)$
3: $\underline{P_b} \leftarrow \min(E_b \cdot S_b \cdot \Delta T, P_b^-)$
4: **if** $S_h \leq \underline{S_h}$ **then**
5: $\quad \widetilde{P_h} \leftarrow E_h \cdot (S_h - S_h \cdot \Delta T \cdot \eta_h)$
6: **else**
7: $\quad \widetilde{P_h} \leftarrow 0$
8: **end if**
9: $P_{\text{net}} \leftarrow P_L - P_G + \widetilde{P_h}$
10: **if** $P_{\text{net}} < 0$ **then**
11: $\quad$ **if** $P_{\text{net}} \leq |\underline{P_b}| \cdot \eta_b$ **then**
12: $\quad\quad p_b \leftarrow -\frac{P_{\text{net}}}{\eta_b}$
13: $\quad\quad p_h \leftarrow \widetilde{P_h}$
14: $\quad$ **else**
15: $\quad\quad p_b \leftarrow \underline{P_b}$
16: $\quad\quad p_h \leftarrow \widetilde{P_h}$
17: $\quad$ **end if**
18: **else**
19: $\quad$ **if** $|P_{\text{net}}| \leq \overline{P_b}$ **then**
20: $\quad\quad p_b \leftarrow -P_{\text{net}} \cdot \eta_b$
21: $\quad\quad p_h \leftarrow \widetilde{P_h}$
22: $\quad$ **else**
23: $\quad\quad p_b \leftarrow \overline{P_b}$
24: $\quad\quad p_h \leftarrow \min\left(\widetilde{P_h} + P_{\text{net}} - \frac{p_b}{\eta_b}, \overline{P_h}\right)$
25: $\quad$ **end if**
26: **end if**

Since the HP cannot discharge, its lower bound is zero. The battery's charging and discharging limits are similarly computed based on its SoC and rated power (**Lines 2–3**). To maintain thermal comfort, the algorithm checks if the TES SoC is below a predefined threshold $\underline{S_h}$ (**Line 4**); if so, the HP is activated to restore it (**Line 5**), otherwise it remains off (**Line 7**). The desired HP power $\widetilde{P_h}$ is then used to calculate the net power balance of the system (**Line 8**). If there is a power deficit ($P_{\text{net}} < 0$), the battery discharges to cover it, either partially or fully, depending on its capacity (**Lines 9–15**). If there is a surplus, the battery charges accordingly (**Lines 16–21**). If the surplus exceeds the battery's charging capacity, the HP increases its consumption to absorb the remaining energy (**Line 22**).

APPENDIX B
VIRTUAL INERTIA

The general control law for virtual or synthetic inertia, in the context of control of power converters, is as follows:

$$P_{emulate} = K_D \omega_{ref} \frac{d\,\Delta\omega}{dt} \tag{1}$$

where $P_{emulate}$ is the power of derivative control, K_D is the inertial proportional conversion gain and ω_{ref} is the nominal grid frequency.

As the grid reacts rapidly to power disturbances, there needs to be a rapid injection of power into the system as a response. For this purpose an idea from a traditional power system, i.e., a second-order active power control from a synchronous generator, can be implemented for a power converter control system. The relationship between the power mismatch and the frequency of a conventional generator can be modeled by the following equations:

$$P_{ref} - P = (Js + K_D).\Delta\omega_{ref} \tag{2}$$

The inertia J of a generator represents its ability to maintain stability and ride through disturbances/power mismatches, and K_D will provide sufficient damping. According to the swing (motion) equation, it quantifies the kinetic energy stored in the rotating mass of the generator, determining its response to changes in electrical load and helping to stabilize the power system.

Figure 15 illustrates the translation of the inertia provided by a conventional generator to a fully electronic converter-based generation system. It defines how to incorporate its inertial behavior using a control law for the conversion system.

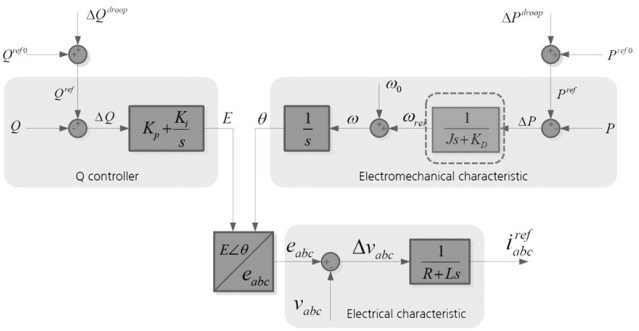

FIGURE 15. Virtual Synchronous Generator-based GFM converter control.

TABLE 6. Components of the modified banshee grid.

Element	Quantity
BESS	1
circuit breakers	55
CHP generator	1
diesel generator	1
distribution transformer	22
feeder protection relays	3
induction motors with compressed loads	2
low-voltage loads	18
medium- and low-voltage line	19
motor/generator controllers	2
power inverter controllers	2
PV system	1
virtual protective relays	50

APPENDIX C
ISLANDING AND LOAD SHEDDING

The architecture LPC Cascaded with Another Protocol Converter has been employed in conjunction to the modified Banshee grid. The list of components in the considered Banshee microgrid are given in the table 6.

In order to verify the prowess of the LPC for standard grid operations such as islanding and load shedding, the following workflow algorithm has been formulated in Algorithm 2:

Algorithm 2 Workflow of Islanding and Load Shedding Use Case

1: $Islandingmode \leftarrow user$
2: $CBF_3 \leftarrow 0$
3: **if** $f_3 < 49.5$ **then**
4: $\quad L_{max} = \max(Loads)$
5: $\quad CBF_{L_{max}} = 0$
6: **end if**

ACKNOWLEDGMENT

The views and opinions expressed are, however, those of the authors only and do not necessarily reflect those of European Union or CINEA. Neither European Union nor the granting authority can be held responsible for them.

REFERENCES

[1] B. Reidenbach, V. Rozite, B. Motherway, P. Henriot, and J. Guyon, "Towards net-zero: Interoperability of technologies to transform the energy system," OECD, Paris, France, Tech. Rep., 2022.
[2] M. Carlier. (Sep. 2024). *Europe: Number of Electric Vehicle Models by Powertrain and Manufacturer 2023*. [Online]. Available: https://www.statista.com/statistics/1419617/europe-number-of-electric-vehicle-models-by-powertrain-and-manufacturer/
[3] J. B. Nørgaard, T. Kerekes, and D. Séra, "Case study of residential PV power and battery storage with the Danish flexible pricing scheme," *Energies*, vol. 12, no. 5, p. 799, Feb. 2019. [Online]. Available: https://www.mdpi.com/1996-1073/12/5/799
[4] *Interoperability*. Accessed: Feb. 3, 2025. [Online]. Available: https://www.cenelec.eu/aboutcenelec/whatwestandfor/societywelfare/interoperability.html
[5] (Mar. 2025). *Interoperability*. [Online]. Available: https://www.entsoe.eu/technopedia/techsheets/interoperability/#:~:text=Interoperability%20is%20the%20ability%20of,interoperability%20applications%20within%20energy%20sectors
[6] *IEEE Standard for Smart Energy Profile Application Protocol*, IEEE Standard 2030.5-2013, 2018.
[7] (2025). *The Role of The IEEE 2030.5 Interoperability Standard In Distributed Energy Resources IntegraTION*. [Online]. Available: https://interstore-project.eu/wp-content/uploads/2025/01/WhitePaper-InterSTORE-final-version.pdf
[8] E. J. Smith, D. A. Robinson, and S. Elphick, "DER control and management strategies for distribution networks: A review of current practices and future directions," *Energies*, vol. 17, no. 11, p. 2636, May 2024. [Online]. Available: https://www.mdpi.com/1996-1073/17/11/2636
[9] A. Veichtlbauer, O. Langthaler, F. P. Andrén, C. Kasberger, and T. I. Strasser, "Open information architecture for seamless integration of renewable energy sources," *Electronics*, vol. 10, no. 4, p. 496, Feb. 2021. [Online]. Available: https://www.mdpi.com/2079-9292/10/4/496
[10] J. Johnson, B. Fox, K. Kaur, and J. Anandan, "Evaluation of interoperable distributed energy resources to IEEE 1547.1 using SunSpec modbus, IEEE 1815, and IEEE 2030.5," *IEEE Access*, vol. 9, pp. 142129–142146, 2021. [Online]. Available: https://ieeexplore.ieee.org/abstract/document/9570300
[11] S. Katipamula, J. Haack, G. Hernandez, B. Akyol, and J. Hagerman, "VOLTTRON: An open-source software platform of the future," *IEEE Electrific. Mag.*, vol. 4, no. 4, pp. 15–22, Dec. 2016. [Online]. Available: https://ieeexplore.ieee.org/abstract/document/7725895
[12] K. P. Schneider et al., "A distributed power system control architecture for improved distribution system resiliency," *IEEE Access*, vol. 7, pp. 9957–9970, 2019. [Online]. Available: https://ieeexplore.ieee.org/abstract/document/8618618
[13] C. Allwardt et al., "VOLTTRON/volttron version 9," VOLTTRON Distrib. Control Syst. Platform, Feb. 2025, doi: 10.11578/dc.20250219.1.
[14] C. S. C. Dande, E. Rakhshani, E. Gümrükcü, A. A. Gil, N. Manuel, D. Carta, A. Lucas, A. Benigni, and A. Monti, "Introduction of legacy protocol converter as an interoperability software," in *Proc. IEEE Int. Conf. Eng., Technol., Innov. (ICE/ITMC)*, Jun. 2025, pp. 1–9.
[15] K. Michal, Š. Michal, and B. Zdeněk, "Interoperability through ontologies," *IFAC Proc. Volumes*, vol. 45, no. 7, pp. 196–200, 2012. [Online]. Available: https://www.sciencedirect.com/science/article/pii/S1474667015350886
[16] H. Lund, N. Duic, P. A. Østergaard, and B. V. Mathiesen, "Smart energy systems and 4th generation district heating," *Energy*, vol. 110, pp. 1–4, Apr. 2016.
[17] A. Wein, A. Steinert, J. S. Schwarz, L. Fuentes-Grau, Z. Pan, A. Monti, and A. Nieße, "Developing interoperable ontologies for research data management in the energy domain," 2024.
[18] F. S. Nepsha, A. A. Nebera, A. A. Andrievsky, and M. I. Krasilnikov, "Development of an ontology for smart distributed energy systems," *IFAC-PapersOnLine*, vol. 55, no. 9, pp. 454–459, 2022. [Online]. Available: https://www.sciencedirect.com/science/article/pii/S2405896322004645
[19] J. P. McCrae, C. Tiberius, A. F. Khan, I. Kernerman, T. Declerck, S. Krek, M. Monachini, and S. Ahmadi, "The ELEXIS interface for interoperable lexical resources," in *Proc. 6th Biennial Conf. Electron. Lexicography (eLex)*, 2019.
[20] U. Herberg, D. Mashima, J. G. Jetcheva, and S. Mirzazad-Barijough, "OpenADR 2.0 deployment architectures: Options and implications," in *Proc. IEEE Int. Conf. Smart Grid Commun. (SmartGridComm)*, Nov. 2014, pp. 782–787.
[21] Z. Jingxi, C. Min, W. Ling, Y. Lixia, P. Shixiong, and L. Dong, "Research on architecture of automatic demand response system based on OpenADR," in *Proc. China Int. Conf. Electr. Distrib. (CICED)*, China, Sep. 2018, pp. 2984–2988.

[22] (2025). (2025). *NATS—Connective Technology for Adaptive Edge & Distributed Systems*. [Online]. Available: https://nats.io/
[23] (2023). (2023). *Legacy Systems Protocol Converter for IEEE2030.5*. [Online]. Available: https://github.com/Horizont-Europe-Interstore/Legacy-Protocol-Converter
[24] (2023). *InterSTORE—Interoperable Open-Source Tools to Enable Hybridisation, Utilisation, and Monetisation of Storage Flexibility*. [Online]. Available: https://interstore-project.eu/
[25] D. Liu, D. Carta, A. Xhonneux, D. Müller, and A. Benigni, "Short-term control of heat pumps to support power grid operation," *IEEE Open J. Ind. Electron. Soc.*, vol. 5, pp. 1221–1238, 2024.
[26] L. Westphal, M. Schröder, D. Carta, A. Xhonneux, A. Benigni, and D. Müller, "Development and application of a FIWARE-based ICT-platform for multi-energy systems on building and district level," in *Proc. Open Source Model. Simul. Energy Syst. (OSMSES)*, Sep. 2024, pp. 1–6.
[27] E. Rakhshani, J. M. Ruiz, X. Benavides, and E. Dominguez, "Enhancing low-inertia power systems with grid forming based hybrid energy storage technology," in *Proc. 12th Int. Conf. Smart Grid (icSmartGrid)*, May 2024, pp. 464–468.
[28] J. M. Ruiz, E. Rakhshani, X. Benavides, and E. Dominguez, "Synergistic multi-service operation of hybrid energy storage systems," in *Proc. 12th Int. Conf. Smart Grid (icSmartGrid)*, May 2024, pp. 469–474.
[29] (2023). *LPC Generator*. [Online]. Available: https://sunesis.si/interstore/lpc/
[30] M. Pau, M. Mirz, J. Dinkelbach, P. Mckeever, F. Ponci, and A. Monti, "A service oriented architecture for the digitalization and automation of distribution grids," *IEEE Access*, vol. 10, pp. 37050–37063, 2022.
[31] P. Kannisto, A. Supponen, S. Repo, and D. Hästbacka, "Electricity system built on cyber-physical enterprises: Architecture analysis," *IFAC-PapersOnLine*, vol. 56, no. 2, pp. 8197–8202, 2023.
[32] P. Raux-Defossez, N. Wegerer, D. Pétillon, A. Bialecki, A. G. Bailey, and R. Belhomme, "Grid services provided by the interactions of energy sectors in multi-energy systems: Three international case studies," *Energy Proc.*, vol. 155, pp. 209–227, Nov. 2018. [Online]. Available: https://www.sciencedirect.com/science/article/pii/S1876610218310099
[33] *SMP Substation Automation Platform*. Accessed: Apr. 29, 2025. [Online]. Available: https://www.eaton.com/us/en-us/catalog/utility-and-grid-solutions/smp-gateway-automation-platform.html
[34] (Mar. 2023). *AEMO*. [Online]. Available: https://aemo.com.au/-/media/files/initiatives/engineering-framework/2023/inertia-in-the-nem-explained.pdf?la=en
[35] (Sep. 2024). *AEMO*. [Online]. Available: https://aemo.com.au/-/media/files/initiatives/engineering-framework/2024/quantifying-synthetic-inertia-from-gfm-bess.pdf
[36] (Nov. 2024). *AEMO*. [Online]. Available: https://www.neso.energy/document/346996/download
[37] K. Malekian, E. Quitmann, T. Bülo, J. Massmann, M. Schmieg, and C. Wulkow, "Requirements and verification procedures for grid-forming units—The German approach to ensure power system stability under very high penetration of inverter-based sources," *IET Conf. Proc.*, vol. 2024, no. 16, pp. 796–804, Feb. 2025.
[38] (2024). *ERCOT*. [Online]. Available: https://www.ercot.com/files/docs/2024/07/10/202407ERCOTIBRWGAdvanced%20Grid%20Support%20Inverter-Based%20ESR%20Functional%20Specification%20and%20Test%20Frameworkv1.pdf
[39] B. Tan, J. Zhao, M. Netto, V. Krishnan, V. Terzija, and Y. Zhang, "Power system inertia estimation: Review of methods and the impacts of converter-interfaced generations," *Int. J. Electr. Power Energy Syst.*, vol. 134, Jan. 2022, Art. no. 107362. [Online]. Available: https://www.sciencedirect.com/science/article/pii/S0142061521006013
[40] R. Salcedo et al., "Banshee distribution network benchmark and prototyping platform for hardware-in-the-loop integration of microgrid and device controllers," *J. Eng.*, vol. 2019, no. 8, pp. 5365–5373, Aug. 2019. [Online]. Available: https://ietresearch.onlinelibrary.wiley.com/doi/abs/10.1049/joe.2018.5174
[41] S. Vogel, N. Eiling, M. Pitz, A. Bach, M. Stevic, and P. A. Monti, "VILLASnode: An open-source real-time multi-protocol gateway," *J. Open Source Softw.*, vol. 10, no. 112, p. 8401, Aug. 2025, doi: 10.21105/joss.08401.
[42] A. Mazza et al., "On the model flexibility of the geographical distributed real-time co-simulation: The example of ENET-RT lab," *Sustain. Energy, Grids Netw.*, vol. 40, Dec. 2024, Art. no. 101501. [Online]. Available: https://www.sciencedirect.com/science/article/pii/S2352467724002303

CHANDRA SEKHAR CHARAN DANDE received the B.Tech. degree in electrical and electronics engineering and the M.Sc. degree in energy science and technology from ETH Zürich, Zürich, Switzerland, in 2021 and 2024, respectively. He is currently pursuing the Ph.D. degree with the E.ON Energy Research Center, Institute for Automation of Complex Power Systems (ACS), RWTH Aachen University, Aachen, Germany. He is a Research Associate with the E.ON Energy Research Center, Institute for Automation of Complex Power Systems (ACS), RWTH Aachen University. His research interests include dynamic simulations, grid control, and energy digitalization.

DANIELE CARTA (Member, IEEE) received the B.Sc., M.Sc., and Ph.D. degrees in electrical engineering from the University of Cagliari, Cagliari, Italy, in 2013, 2016, and 2020, respectively.

He is currently with the Department Leader of the "Control Solution" Group, "Institute of Climate and Energy Systems: Energy Systems Engineering (ICE-1)", Forschungszentrum Jülich.

ERDEM GÜMRÜKCÜ (Member, IEEE) received the B.Sc. degree in electrical engineering from Istanbul Technical University and the M.Sc. and Ph.D. degrees in electrical power engineering from RWTH Aachen University. From 2018 to 2023, he was a Research Associate with the Institute for Automation of Complex Power System, E.ON Energy Research Center. In 2024, he joined Eaton as the Lead Engineer in energy systems. In this role, he worked on several research projects on electric vehicle charging optimization and local energy communities. He is currently conducting research on energy flexibility management, smart grids, and digitalization.

ELYAS RAKHSHANI (Senior Member, IEEE) received the B.Sc. degree in power systems, the master's degree in control systems, and the Ph.D. degree (cum laude) in electrical engineering from the Universitat Politécnica de Catalunya (UPC), Barcelona, Spain, in 2004, 2008, and 2016, respectively. He is currently a Senior Control and Power Systems Engineer, leading the Algorithm and Control Group, HESSTec Company, Spain, with a focus on dynamic low-inertia grids, hybrid energy storage integration. His research interests include modern power system control, dynamic stability, hybrid energy storage integration, converter control applications in power systems, HVDC control for grid applications, and frequency control. He is a member of the Editorial Board of Power and Energy Society (PES) journals, such as IEEE Transactions on Power Systems, IEEE Power Engineering Letters, *IET Generation Transmission and Distribution*, *IET Renewable Power Generation*, and IEEE Systems Journal.

ANDRES ACOSTA GIL received the B.Sc. degree in telecommunications engineering from Universidad Pontificia Bolivariana, Medellín, in 2012, and the M.Sc. degree in systems engineering from the Universidad Nacional de Colombia, Medellín, in 2017, where he is currently pursuing the Ph.D. degree. From 2013 to 2022, he was a Research Assistant with the Applied Mathematics line of the Automation Group of Universidad Nacional (GAUNAL). Since 2023, he is a Research Associate with E.ON Energy Research Center, Institute for Automation of Complex Power Systems (ACS), RWTH Aachen University. His main research interests include dynamical systems, computer simulation, convex optimization, and model predictive control.

NITHIN MANUEL received the B.Tech. degree in electronics and communication Engineering and the master's degree in telecommunications engineering from the University of Parma, Parma, Italy, in 2013 and 2018, respectively. He is currently a Software Developer with the E.ON Energy Research Center, Institute for Automation of Complex Power Systems (ACS), RWTH Aachen University, Aachen, Germany. His interests include communication protocols and interoperability.

ALEXANDRE LUCAS received the Electrical Engineering degree from ISEL, in 2007, the master's degree in business and industrial strategy from ISEG, in 2009, and the Ph.D. degree in sustainable energy systems from IST, in 2013. He developed research at MIT, from 2011 to 2012, and complementary training at Harvard on Energy Management. With nine years of experience in power substations, he joined European Commission, in 2014, working for the JRC until 2020. He then joined INESC TEC, dedicated to research and innovation projects. Reference projects are Electra, Delta, Drimpac, Interconnect, OneNet, COSMIC, InterStore, Every1, and EnerTEF. His research focuses on energy digitalization, energy management, demand response, and distributed energy resource integration.

ANDREA BENIGNI (Senior Member, IEEE) received the B.Sc. and M.Sc. degrees from the Politecnico di Milano, Milan, Italy, in 2005 and 2008, respectively, and the Ph.D. degree from RWTH Aachen University, Aachen, Germany, in 2013.

From 2014 to 2019, he was an Assistant Professor with the Department of Electrical Engineering, University of South Carolina, Columbia, SC, USA. Since 2019, he is currently a Full Professor with RWTH Aachen, and the Director of the ''Institute of Climate and Energy Systems: Energy Systems Engineering (ICE-1)'', Forschungszentrum Jülich.

ANTONELLO MONTI (Senior Member, IEEE) received the M.Sc. (summa cum laude) and Ph.D. degrees in electrical engineering from the Politecnico di Milano, Milan, Italy, in 1989 and 1994, respectively. He started his career with Ansaldo Industria and then moved to the Politecnico di Milano as an Assistant Professor, in 1995. In 2000, he joined the Department of Electrical Engineering, University of South Carolina, Columbia, SC, USA, as an Associate Professor and later became a Full Professor. Since 2008, he has been the Director of the Institute for Automation of Complex Power Systems, E.ON Energy Research Center, RWTH Aachen University, Aachen, Germany. Since 2019, he has been a joined appointment at Fraunhofer FIT within the Center for Digital Energy Aachen. He has authored or co-authored more than 400 peer-reviewed papers published in international journals and in the proceedings of international conferences. He is a member of the Editorial Board of *Sustainable Energy, Grids and Networks* and the Founding Board of *Energy Informatics*. He was a recipient of the 2017 IEEE Innovation in Societal Infrastructure Award. He is an Associate Editor for *IEEE Electrification Magazine*.